European Polymer Journal 64 (2015) 70–78

Contents lists available at ScienceDirect

European Polymer Journal

journal homepage: www.elsevier.com/locate/europolj

A simple and effective method to ameliorate the interfacial properties of cellulosic fibre based bio-composites using poly (ethylene glycol) based amphiphiles

Jeffrey S. Church [b], Andreea S. Voda [a], Alessandra Sutti [a], John George [a], Bronwyn L. Fox [a], Kevin Magniez [a,*]

[a] Institute for Frontier Materials, Deakin University, Waurn Ponds, 3217, Australia
[b] CSIRO Materials Science and Engineering, Waurn Ponds, 3217, Australia

ARTICLE INFO

Article history:
Received 29 August 2014
Received in revised form 23 November 2014
Accepted 13 December 2014
Available online 23 December 2014

Keywords:
Bio-composite
Surface treatment
Fibre–matrix interface
Amphiphiles

ABSTRACT

In order to overcome interfacial incompatibility issues in natural fibre reinforced polymer bio-composites, surface modifications of the natural fibres using complex and environmentally unfriendly chemical methods is necessary. In this paper, we demonstrate that the interfacial properties of cellulose-based bio-composites can be tailored through surface adsorption of polyethylene glycol (PEG) based amphiphilic block copolymers using a greener alternative methodology. Mixtures of water or water/acetone were used to form amphiphilic emulsions or micro-crystal suspensions of PEG based amphiphilic block copolymers, and their deposition from solution onto the cellulosic substrate was carried out by simple dip-coating. The findings of this study evidence that, by tuning the amphiphilicity and the type of building blocks attached to the PEG unit, the flexural and dynamic thermo-mechanical properties of cellulose-based bio-composites comprised of either polylactide (PLA) or high density polyethylene (HDPE) as a matrix, can be remarkably enhanced. The trends, largely driven by interfacial effects, can be ascribed to the combined action of the hydrophilic and hydrophobic components of these amphiphiles. The nature of the interactions formed across the fibre–matrix interface is discussed. The collective outcome from this study provides a technological template to significantly improve the performance of cellulose-based bio-composite materials.

1. Introduction

Current environmental concerns and stricter regulations throughout the world have led to a wide shift towards the design of engineering materials using ecologically-friendly and sustainable manufacturing methodologies. In this context, the use of renewable materials such as natural fibres in commodity composites has rapidly increased over the past few years and more recently natural fibres have become one of the fastest growing filler and reinforcing materials for thermoplastics [1]. Bio-composites which are derived from the combination of natural fibres with a thermoplastic (or a thermoset) have been used for a number of applications in the automotive, building and packaging sectors [2,3].

However, the implementation of natural fibres as an alternative reinforcement to synthetic fibres in the design of structural engineering composites has been hindered by limitations relating to the long term structural and functional stability of these materials. The lack of

* Corresponding author at: Institute for Frontier Materials, Deakin University, Geelong, Australia. Tel.: +61 3 5227 1305.
E-mail address: kevin.magniez@research.deakin.edu.au (K. Magniez).

http://dx.doi.org/10.1016/j.eurpolymj.2014.12.024
0014-3057/

performance essentially stems from the poor interfacial quality between the hydrophilic natural fibre and the hydrophobic polymer. To date, the primary avenue of research employed to tackle this interfacial compatibility issue has been focussed on the surface modifications of the natural fibres using chemical routes including alkali, silanization, acetylation, graft co-polymerization, etherification and maleated-polypropylene [1,2,4–8] or physical plasma routes [9–12]. The chemical surface modification often improves the hydrophobicity of the fibre surface, thus promoting interfacial bonding via diffusion of the chain segments into the matrix [13]. The chemical surface pre-treatment of natural fibres is typically carried out separately, prior the processing of the composites, and involves a number of successive steps [14,15]. The surface functionalised fibres can be used to reinforce thermoplastic or thermoset resins by injection moulding, compression moulding, extrusion, sheet moulding compound (SMC) or resin transfer moulding (RTM) techniques [16,17]. Nonwovens, typically produced by carding of natural fibres with a thermoplastic fibre (often polypropylene), are consolidated into a bio-composites for automotive interior applications by compression moulding [17]. The surface modification of natural fibres has also been reported by means of reactive extrusion via grafting of di-functional coupling agents such as anhydrides, isocyanates or benzophenone onto the natural fibres [15,18]. The resulting fibre/thermoplastic blend can be turned into a product using compression moulding or injection moulding.

Whilst these methods were found to be effective to some extent, one could argue that in an ecologically-friendly manufacturing context, the reported methods are not really acceptable as most methods use a range of toxic chemicals, involve multi-step reactions and are not energy efficient.

In our previous work, we presented the possibility of overcoming the interfacial affinity issues in a jute/polylactide (PLA) bio-composite by deposition of PEG–PLLA amphiphilic block copolymers from solution [19]. This method offered some environmental benefits as in most cases water/acetone mixtures were used to treat the surface of the fibrous substrate. We found that strong interactions, such as intra- and inter-molecular hydrogen bonds formed across the fibre–matrix interface, induced a certain degree of enhancement in properties in these bio-composites.

The work presented here extends on this concept by looking into tuning both the amphiphilicity and the nature of the building blocks constituting the copolymers in order to optimize the performance of the cellulose based bio-composite, for which the matrix is either PLA or high density polyethylene (HDPE). These particular matrices were chosen because PLA is of high interest due to its sustainability and bio-derived nature whilst polyolefin polymers such as HDPE are still highly utilized for industrial applications such as automotive [3,20] and construction [21] due to their lower cost. The current work builds on the previously reported concept that poly (ethylene glycol) (PEG) has tremendous potential for forming hydrogen bonding interactions with cellulose [22,23], and will use exclusively amphiphilic copolymers having either $C_{18}H_{35}$ or a polyethylene (PE) block attached to a PEG block. This research paper will investigate their deposition from solution and surface adsorption onto the cellulosic substrate. The effects of both the block type and the amphiphilicity of the copolymers on the properties of the corresponding cellulose based bio-composites will be analysed and the nature of the interactions across the interface will be discussed.

2. Materials and experimental procedures

2.1. Materials

A plain weave of cellulose (regenerated bamboo *Corchorus genus*) fabric of approximately 150 g/m^2 was obtained from Bamboo Australia.

Polylactic acid films (300 μm in thickness) were purchased from Bi-Ax International (Canada). High density polyethylene films (HD5148, 300 μm in thickness) were kindly donated by Qenos Australia.

Three poly (ethylene glycol)-*block*-oleyl ether copolymers (Brij® 93, O10 and 98) were obtained from Sigma Aldrich. In these copolymers, referred to herein as PEG_n–*b*–C_{18}, the number of PEG units, *n*, are 2, 10 and 20 and their hydrophilic–lipophilic balance (HLB) values are 4, 12 and 15, respectively.

Three polyethylene-*block*-poly (ethylene glycol) copolymers of average $M_n \sim 1400$ g/mol, 920 g/mol and $M_n \sim 875$ g/mol were obtained from Sigma Aldrich. These copolymers will be referred to herein as PEG_p–*b*–PE_m, the number of polyethylene units *m* is 25, 17 and 25 whilst the number of PEG units is *p* is 16, 10 and 4, respectively. Their HLB values are 10, 10 and 4, respectively.

2.2. Surface treatment of the cellulosic substrate

The first step involved looking at the solubility of each copolymer in preferably water but also in mixtures of water and acetone. The fabrics were then surface coated with 2.5 weight percent (wt%) of each copolymer. The solvent uptake was calculated for each mixture by taking the average weight absorbed by the fabric after dipping the fabric into a glass beaker filled with a large quantity of each solvent mixture. Surface treatment was carried out by dipping once for approximately 2 min, square samples of known dimensions and mass into solutions containing various concentrations of copolymer (which generally varied between 10 and 15 g/L solvent). The fabrics were then dried *in vacuo* at 80 °C for 12 h.

2.3. Fabrication of the bio-composites

The treated fabrics were used to produce composite samples with PLA and HDPE films. In order to minimise hydrolysis of the polymer chains caused by a combination of moisture and heat, the PLA films were dried overnight *in vacuo* at 80 °C prior to processing. HDPE being very hydrophobic was used as received without any drying. The composites were produced by compression moulding via a stacking procedure using square samples of fabrics (120 mm in length). The stacking sequence was achieved

by alternating four layers of fabrics with five layers of films (PLA or HDPE). The stack was placed into a stainless steel mould coated with a release agent. The assembly was vacuum bagged at 85 kPa and placed in a hot press at 175 °C for 5 min. Pressures of 1.5 MPa for 2.5 min followed by 2.5 MPa for 2.5 min were applied respectively. The composites were removed from the press, de-bagged and immediately annealed in a conventional oven at 110 °C for 30 min. A complete schematic of the fabrication procedure used in this work is presented in Fig. 1.

2.4. Characterisation

2.4.1. Optical microscopy

Optical micrographs were taken in reflection mode using an Olympus DP71 digital camera at 5–10× total magnification using a few drops of solution deposited on a glass slide. A Nomarski-type filter was applied to evidence phases of different refractive index.

2.4.2. Raman and infra-red spectroscopy

Raman spectra and spectral maps were obtained using an inVia confocal microscope (Renishaw, Gloucestershire, UK) equipped with the Streamline Plus chemical imaging system. The Raman shifts were calibrated using the 520 cm^{-1} line of a silicon wafer. The spectral resolution was ~1 cm^{-1}. The 514 nm excitation from an argon ion laser (Modu-Laser Stellar-Pro ML/150) through a 50× (0.75 na) objective gave an incident laser power of 4.5 mW at the sample as measured using an Ophir Nova power meter fitted with a PD300-3W photodiode head. This laser power gave good signal to noise spectra and was found not to have any adverse effects on the samples. All samples were mounted on mirrored surfaces. The fibre bundles within the fabrics were orientated parallel to the polarization of the laser with the aid of a rotating stage. Raman survey scans were obtained by averaging 4 accumulations, each with a 20 s exposure time. Raman spectral maps were collected in highly confocal mode over an area approximately 10 × 10 μm, using 1 μm increments between data points, giving a total number of data points per map of 121. Each spectrum was a single static accumulation with a 35 s exposure time over the range of 544–1837 cm^{-1}.

False colour maps were created using WiRE software version 3.4 (Renishaw, Gloucestershire, UK). The spectral region between 950 and 865 cm^{-1} was deconvoluted into two components at 926 and 897 cm^{-1} which were identified through 2nd derivative spectroscopy. The region between 1300 and 1286 cm^{-1} was fitted with one band at 1295 cm^{-1}. The 897 cm^{-1} band is due to the cellulose fabric while the 1295 cm^{-1} band can be attributed to the PEG_2–*b*–C_{18}. Fits were based on band components represented by a variable mixture of Gaussian and Lorentzian functions. All peak heights were limited to the range greater than or equal to zero. In the initial fitting steps the frequencies of overlapping band centres were only allowed to vary by ±5 cm^{-1} from the frequency determined by the second derivative spectra. All Raman maps were translated onto the same colour scale through the use of a look up table.

Infrared attenuated total reflectance (ATR) spectra were collected from the films using a Perkin Elmer (Beaconsfield, UK) System 2000 Fourier transform infrared (FTIR) spectrometer fitted with single bounce Ge Pike Technologies MIRacle ATR accessory (Madison, USA) and a liquid nitrogen cooled Mercury Cadmium Telluride detector. Spectra were collected at 4 cm^{-1} resolution with 64 scans co-added. All spectroscopic data manipulation was carried out using Grams AI V 9.1 software (Thermo Fisher Scientific, Waltham, USA).

2.4.3. Differential scanning calorimetry

The thermal properties of the materials were investigated using a TA Instruments Q200 operated under a nitrogen stream at a flow rate of 20 mL/min using sealed aluminium pans.

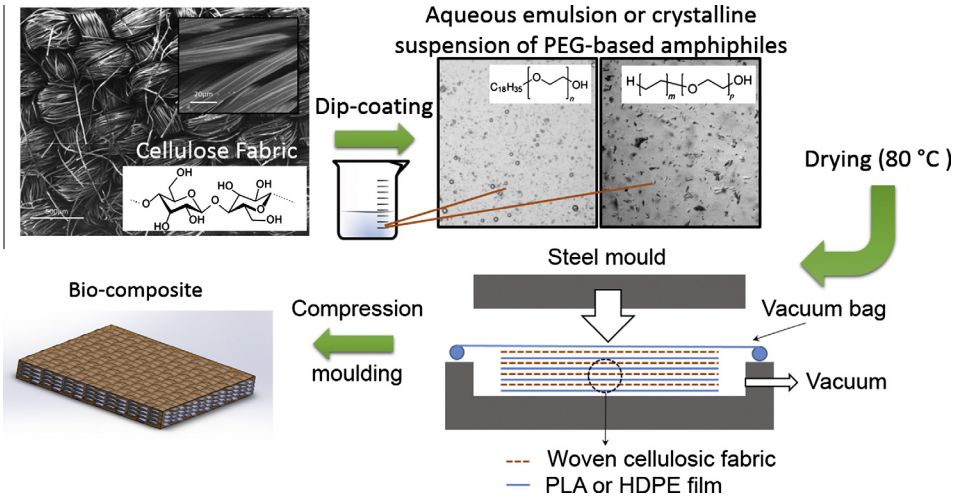

Fig. 1. Schematic representation of the bio-composites fabrication procedure.

2.4.4. Mechanical properties of the bio-composites

Dynamic mechanical analyses (DMA) were performed using a Q800 instrument equipped in dual-cantilever mode using a frequency of 1 Hz with a constant strain of 0.05% and a heating rate of 2 °C/min between 0 and 125 °C. Specimens of approximate dimensions of 55 mm × 12 mm × 2 mm were used. Flexural strength and flexural modulus were determined on a Lloyd LR30 K universal tensile tester using the 3 point bending method as per ASTM D790-84a with a span length of 16 times the thickness and a crosshead speed of 2 mm/min. All tests were conducted at 20 ± 2 °C and 65 ± 2% relative humidity.

3. Results and discussion

3.1. Cellulose/PLA bio-composites

It is important to first discuss the solution properties of the amphiphilic copolymers and their surface deposition onto the cellulosic substrate, prior to fabricating the composites. The hydrophilic–lipophilic balance (HLB) values for the PEG_{10}–*b*–C_{18} and PEG_{20}–*b*–C_{18} copolymers are 12 and 15, respectively, indicating that these copolymers have a stronger hydrophilic character. These copolymers are water soluble and thus when dispersed in water the solutions are visually clear (Supplementary Information, Fig. SI1-A). On the other hand, the PEG_2–*b*–C_{18} copolymer has a much lower HLB value of 4 and is lipid-soluble due to its stronger hydrophobic character. This copolymer, liquid at room temperature, disperses in a water/acetone solution (3–1 ratio) yielding a fine oil in water emulsion that is milky in appearance. The droplets are approximately between 5 and 30 μm in size (Supplementary Information, Fig. SI1-B). The emulsion was found to be quite stable; the image in Fig. SI1-B was taken 48 h after mixing.

After deposition and surface adsorption of all the copolymers onto the cellulosic fabric via dip coating from these solutions, the presence of the copolymers was not detectable in the Raman spectra of the cellulosic fabric (Supplementary Information, Fig. SI2). The low wavenumber Raman spectra obtained from the PEG_2–*b*–C_{18} and cellulose fabric are shown as traces A and B in Fig. SI2 (Supplementary Information) respectively. A typical spectrum obtained after treatment of the fabric with the PEG_2–*b*–C_{18} copolymer is shown as trace C. The strongest feature in the low wavenumber Raman spectrum obtained from PEG_2–*b*–C_{18} is the 1655 cm^{-1} band which is assigned to the C=C stretching vibration in the C_{18} chain [24]. This feature could not be detected in any of the spectra obtained from the treated fabric suggesting that the PEG_2–*b*–C_{18} is present as a very thin coating on the fibre surface. As it has been aforementioned that all PEG–*b*–C_{18} copolymers studied in this work were deposited onto the fabric in a liquid form and local migration of the copolymers is to be anticipated within the cellulose substrate after drying of the fabric.

The presence of the copolymer within the top surface of the cellulosic substrate was verified through ATR-FTIR spectra analysis of thePEG_2–*b*–C_{18}, cellulose fabric and PEG_2–*b*–C_{18} treated fabric (shown in Fig. 2 as traces A, B and C, respectively). Careful comparison of the spectra revealed several differences in the absorbance pattern that can be attributed to the presence of PEG_2–*b*–C_{18}. CH_2 stretching vibrations associated with CH_2–O groups are observed at 2918 and 2847 cm^{-1} and the CH_2 deformation is observed at 1457 cm^{-1}. The asymmetric C–O–C stretching vibration observed at 1111 cm^{-1} in the spectrum obtained from the PEG_2–*b*–C_{18} (trace A) is masked by the strong C–O modes of the cellulose molecules [24]. As the depth of penetration of the evanescent wave into the cellulose at 2900 cm^{-1} can be estimated to be of the order of 0.23 μm it is likely that a thin uniform layer of PEG_2–*b*–C_{18} is on the surface of all fibres (below the limit of detection of the less surface sensitive Raman technique) [25]. To further investigate the presence of PEG_2–*b*–C_{18} on the fabric surface the spectrum obtained from the residue left on the Ge ATR crystal after the treated fabrics was removed was recorded. This spectrum, shown as trace A is Fig. SI3 (Supplementary Information), is in excellent agreement with that of the pure PEG_2–*b*–C_{18} shown as trace B. Furthermore, the scale factor of 26 used in this plot high lights the thin amount of PEG_2–*b*–C_{18} present on the surface of the fibres.

The quasi-static flexural results presented in Fig. 3 point out that the surface treatment of the cellulosic substrate using the various PEG–*b*–C_{18} amphiphiles had a positive influence on both the flexural modulus and strength of the bio-composites with some noticeable enhancements. The effects of the PEG block length was quite obvious in Fig. 3. Whilst the copolymers containing the higher PEG chain lengths of 10 or 20 provided a very reasonable improvement (~25% in flexural modulus and ~15% in flexural strength), the copolymer containing the shortest PEG chain, PEG_2–*b*–C_{18} (HLB of 4), displayed the best performance with improvements of 54% and 47% in flexural modulus and strength. This improvement is higher than what we previously reported using PEG–PLLA amphiphiles having a minimum HLB of approximately 7 [19]. Clearly the PEG_2–*b*–C_{18} copolymer shows the strongest hydrophobic character and provided the greatest improvement to the PLA–cellulose interface than the PEG_{20}–*b*–C_{18} and PEG_{10}–*b*–C_{18} copolymers with lower hydrophobic character.

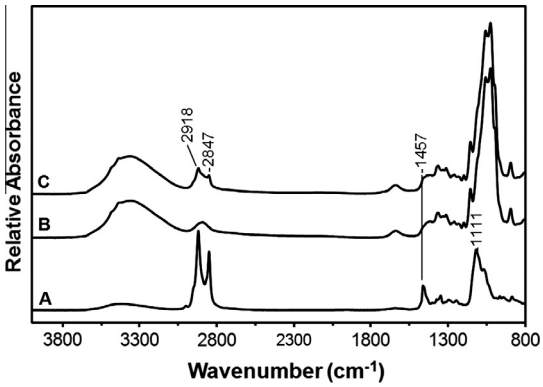

Fig. 2. Infrared ATR spectra obtained from (A) PEG_2–*b*–C_{18}, (B) cellulose fabric and (C) PEG_2–*b*–C_{18} treated fabric.

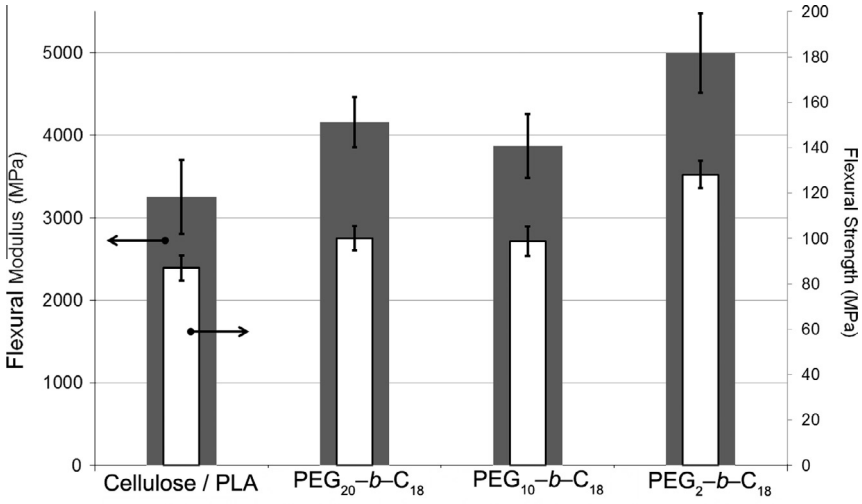

Fig. 3. Effect of surface treatment of the cellulosic substrate using PEG_n–*b*–C_{18} on the flexural properties of the corresponding composites with PLA.

Moreover, polyethylene glycols are known to be highly flexible and hydrophilic polymers [26] and have been shown to form strong hydrogen bonds when in contact with cellulose [22,23]. Consequently, and in light of our results, it can be postulated that the shorter PEG chains allowed for lower degrees of slipping and hydrogen bonding dissociation and restructuring at the cellulose–PEG interface than do the longer PEG chains. However, the improvement in interfacial properties can most likely be ascribed to the combined action of the hydrophilic PEG and hydrophobic C_{18} components.

It has been previously reported that in a fibre reinforced composite, the interfacial properties between the matrix and the fibre correlate well to their dynamic properties [27–29]. The dynamic and thermal analysis data presented in Fig. 4 supports this assumption. Over the range of temperatures tested, the dynamic response of the bio-composites was greatly ameliorated after treatment with the various amphiphiles, in line with the improved fibre–matrix adhesion. An analysis of the data indicates that at room temperature, the composite performs better with the adsorption of the PEG_2–*b*–C_{18} system for which the storage modulus was found to be 60% higher than the untreated cellulose bio-composite, correlating well with the static flexural modulus data. Further, the observed shift in the peak of tan delta (T_g) of 4.5 °C coupled with a reduction in the height of the tan δ curve reflects on a restriction of the molecular mobility at the interface and improved interaction at the fibre–matrix interface as reported elsewhere [30].

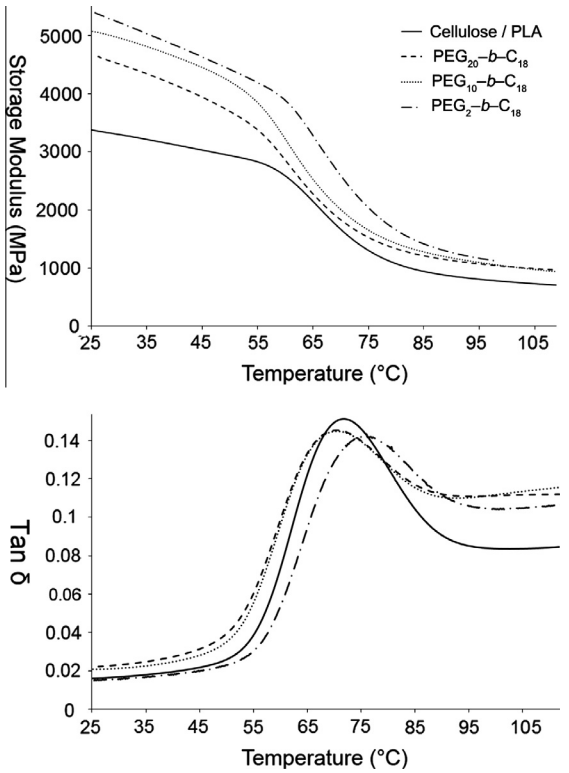

Fig. 4. Effect of surface treatment of the cellulosic substrate using PEG_n–*b*–C_{18} copolymers on the storage modulus (top) and tan δ (bottom) properties of the corresponding composites with PLA.

3.2. Cellulose/HDPE bio-composites

In the next set of experiments a non-polar polyolefin HDPE homopolymer matrix was used. The cellulose fabrics were treated with the PEG_2–*b*–C_{18} (which provided the best result with a PLA matrix in the previous section) and with three polyethylene-*block*-poly (ethylene glycol) copolymers: PEG_{16}–*b*–PE_{25}, PEG_{10}–*b*–PE_{17} and PEG_4–*b*–PE_{25}. In the latter types of block copolymer, the block attached to the PEG unit is identical to the polyethylene matrix. In doing so, it was possible to separate and independently analyse the effects that the type (e.g. PE vs C_{18}) and length of the PE block attached to the PEG unit have on the interfacial and physical properties of the resulting composites.

In relation to their solution properties, none of the PEG–*b*–PE copolymers are water soluble and therefore mixtures of water/acetone (3–1 ratios) were employed to form cloudy dispersions which were subsequently used for dip-coating of the fabrics. Under the optical microscope, the suspension containing the PEG_{16}–*b*–PE_{25} and the PEG_{10}–*b*–PE_{17} copolymer presented uniformly dispersed particles throughout the volume (Fig. SI4-A and B, Supplementary Information). On the other hand, the PEG_4–*b*–PE_{25} copolymer suspension presented crystalline precipitates floating on the aqueous surface, indicating their more pronounced hydrophobic character (Fig. SI4-C).

Because the PEG–*b*–PE copolymer solutions consisted of solid particles or suspensions of micro-crystals, it was important to understand how the copolymers were deposited and adsorbed onto the fabric after the dip coating process. We therefore investigated the homogeneity of the deposition using Raman spot analysis (0.8 μm in diameter) over a broad area of the treated fabric. The spectra obtained from the PEG_4–*b*–PE_{25} and cellulose fabric are shown as traces A and B of Fig. SI5 (Supplementary Information), respectively. Typical low wavenumber Raman spectra obtained from the PEG_4–*b*–PE_{25} treated fabric are shown as traces C and D. All of the spectra obtained from fabric samples were normalised on the 897 cm^{-1} band that is associated with the β-glycosidic linkages found in cellulose [31]. The sharp bands of the PEG_4–*b*–PE_{25} are clearly evident in trace D but not detectable in trace C. This result suggested that the dispersion of the PEG–*b*–PE is variable with localized areas of thick coverage.

This result was further confirmed through SEM imaging and Raman mapping of the PEG_4–*b*–PE_{25} treated fabric (Fig. 5A and B), where a sparse copolymer dispersion with micron-size crystalline features were visible on the filaments constituting the yarn of the fabric. A Raman chemical functional map representing the distribution of this copolymer over a 10×10 μm randomly chosen area is shown as Fig 5C. The *Y* axis of the Raman map is aligned with the direction of the fibres.

The map colour represents the intensity of the 1295 cm^{-1} copolymer band that can be assigned to the CH_2 twisting vibration of the (—CH_2—) chains in PEG–*b*–PE normalised by the intensity of the 897 cm^{-1} cellulose band. As given by the legend on the right hand side of the figure, black ($I_{1295}/I_{897} = 0$) indicates no polymer detected while white ($I_{1295}/I_{897} \sim 1.6$) represents a maximum amount detected. It can be seen from the map that the PEG_4–*b*–PE_{25} copolymer crystallites were indeed visible at the microscopic level (represented in the map by the large white/yellow entities). Nonetheless, it is important to also highlight that the cellulosic surface was largely covered by thinner deposits of the copolymer (red, $I_{1295}/I_{897} \sim 0.4$) that is beyond what could be seen in the SEM images.

We then looked at the stability of the cellulose–copolymer interaction after subsequent rinsing in water. The previously PEG_4–*b*–PE_{25} treated fabric which was immersed in MiliQ water at room temperature, vigorously stirred for approximately 1 min and re-dried. We found that the presence of PEG_4–*b*–PE_{25} could still be detected on the surface

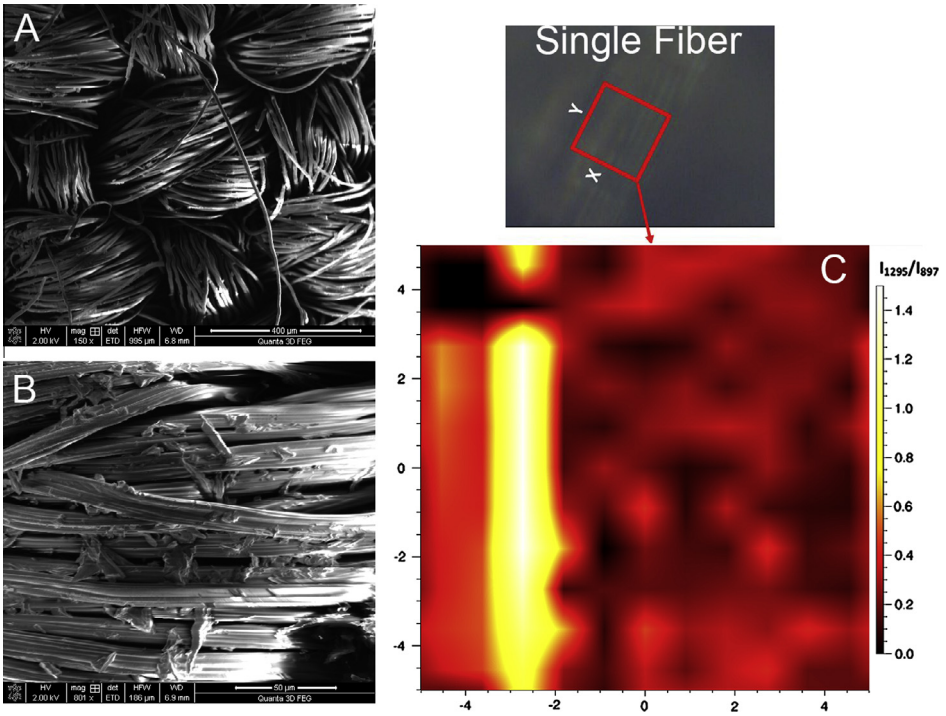

Fig. 5. SEM images of the PEG_4–*b*–PE_{25} treated fabric (A and B) and a 10 by 10 μm Raman chemical functional map (C) showing the presence of copolymer on the surface (black is the substrate, red is the PEG_4–*b*–PE_{25} copolymer). (For interpretation of the references to colour in this figure legend, the reader is referred to the web version of this article.)

as showed in the Raman chemical functional map depicted in Fig. 6A. The larger crystalline structures disappeared but the map clearly indicated the presence of a thin PEG_4–*b*–PE_{25} layer (represented in the map by the red coloured areas). The copolymer distributions obtained from the Raman maps are shown in Fig. 6B. The distribution obtained for the original treated fabric, depicted by the black histogram bars, suggested a broad unevenness in the deposition while after subsequent rinsing and drying the distribution, depicted as the red bars, was found to be narrower and lower in value, suggesting that the dispersion was more uniform and thinner. The molecular interactions at the interface between the thinly distributed microcrystalline species and the cellulose substrate must have been strong enough to overcome the rinsing and stirring process.

The flexural properties of the resulting bio-composite samples are presented in Fig. 7. The trends again show an obvious dependence on the type of surface treatment. The PEG_2–*b*–C_{18} copolymer, which provided the best improvement with a PLA matrix, was only very mildly effective in the HDPE matrix. The enhancement in flexural modulus was 17%, accompanied by a slight (9%) loss in strength (possibly within statistical deviation). On the

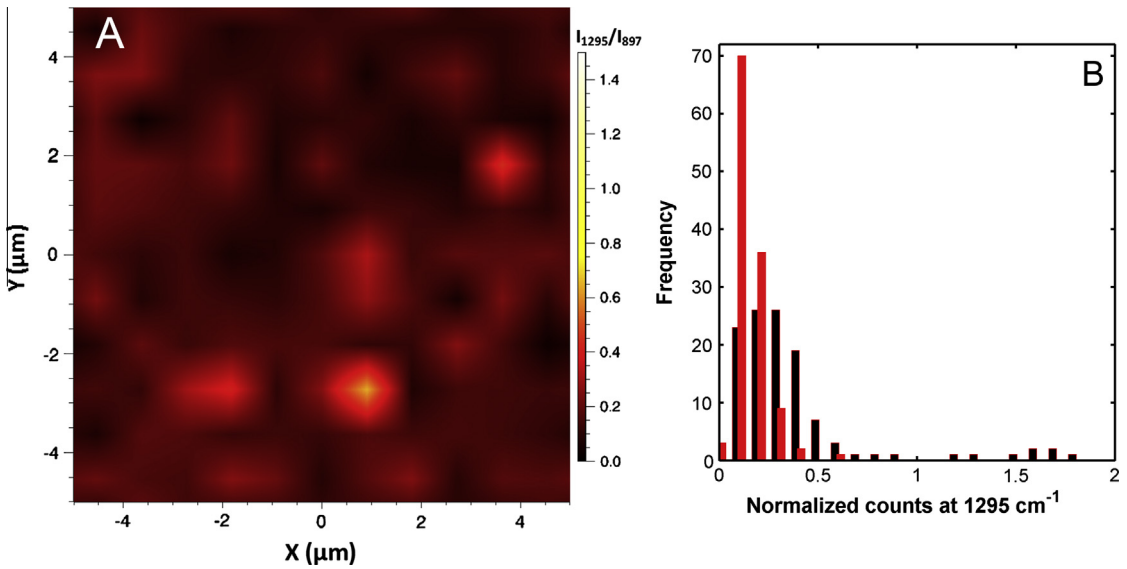

Fig. 6. Raman chemical functional map (10 by 10 μm) after subsequent rinsing of the treated fabric (A) and histogram (B) of PEG_4–*b*–PE_{25} counts derived from the normalised intensity data from the two maps; black is as treated and red is after subsequent rinsing and drying. (For interpretation of the references to colour in this figure legend, the reader is referred to the web version of this article.)

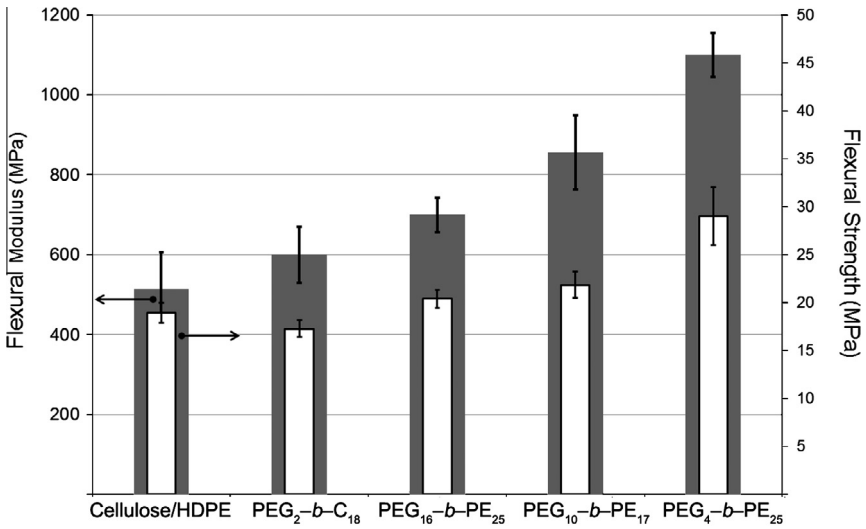

Fig. 7. Effect of surface treatment of the cellulosic substrate using PEG_2–*b*–C_{18} and PEG–*b*–PE on the flexural properties of the corresponding composites with HDPE.

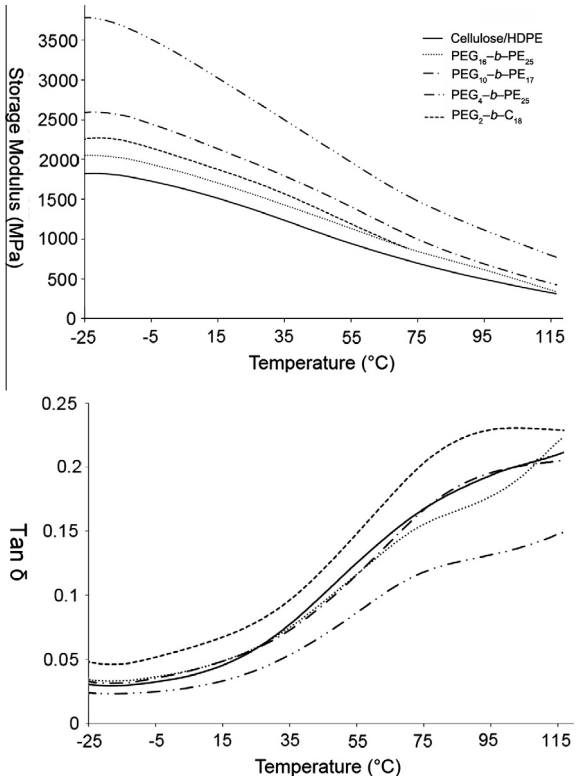

Fig. 8. Effect of surface treatment of the cellulosic substrate using PEG_2–*b*–C_{18} and PEG–*b*–PE on the storage modulus (top) and tan delta (bottom) properties of the corresponding composites with HDPE.

other hand, it is clear from Fig. 7 that the PEG–*b*–PE type copolymers were much more effective at improving the flexural performance of the HDPE composites. The PEG_4–*b*–PE_{25} copolymer clearly outperformed the other systems displaying a remarkable 115% and 54% increase in flexural modulus and strength, respectively. The same conclusions which have been made before in regards to the effect of the hydrophilic/hydrophobic character of the copolymers on the interfacial properties can be also drawn. In addition to this, the trends evidenced that the nature of the block attached to the PEG block is critical in tuning the interfacial properties of the composite. Here the PE block was found to be more effective because firstly it is compatible with the HDPE matrix due to its identical chemical make-up and secondly the possibility of molecular interactions between the PE and HDPE chains through van der Waals bonds also exist. DMTA data was also consistent with the flexural static data, showing a large improvement of up to 125% in the dynamic storage modulus between −25 °C and 115 °C and showing a significant decrease in the height of the tan delta associated with an improved interface (Fig. 8) [30].

The paper investigated alternative explanations for the property improvements observed in this work. The flexural properties of a composite are dictated by the properties of the individual constituents, fibre volume fraction and interfacial strength. In light of the significant improvements in modulus observed in this work, one could argue that the fibre volume fraction between the samples must vary. However it is important to stress that we ensured that the fibre volume fraction remained consistent from sample to sample and minimised this effect to the best of our ability. The cellulosic fabric used was man-made from regenerated bamboo and was very consistent in thickness. The cellulosic fibres constituting the fabric were also very homogenous in diameter (~20 μm from SEM analysis, see Fig. 9). Moreover the pressures (of up to 5 bars corresponding to approximately 2.5 MPa) and temperatures applied to fabricate the composites were consistently the same, yielding composites of approximate thicknesses of 1.8 ± 0.1 mm. In addition vacuum (85 kPa) was applied during fabrication to minimise the presence of voids, which are also inter-related to the flexural performance of a composite. We can thus consider that the fibre volume fraction was relatively consistent between samples.

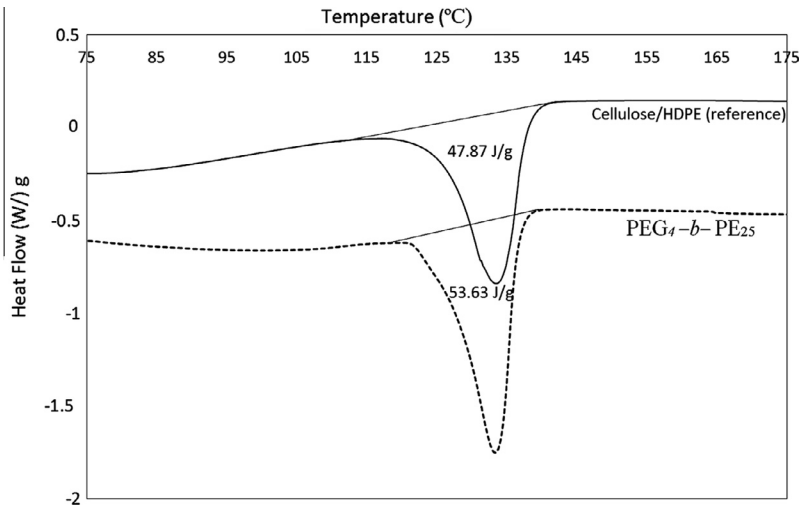

Fig. 9. DSC endotherms for the cellulose/HDPE (top) and PEG_4–*b*–PE_{25} treated cellulose/HDPE samples (only shown here for brevity).

It could be implied that the trends could have been related to significant changes in the crystallinity of the HDPE matrix. However, it is important to note that all samples were annealed at 110 °C for 30 min post-processing prior to the mechanical testing in order to maximise the crystallinity of the HDPE matrix (or PLA matrix in the case of the previous experiments). Regardless of that, the difference in crystallinity between the untreated cellulose/HDPE and the PEG_4–*b*–PE_{25} treated cellulose sample (which displayed the largest improvement) was verified. The DSC dynamic scan of these two samples revealed a heat flow of approximately ~50 J/g ± 5 J/g (Fig. 9) and considering that the heat of fusion of fully crystalline HDPE is 293 J/g [32], it signifies that the difference in crystallinity is less than 2% between samples. This difference cannot be considered significant enough to justify the observed large increase in modulus after treatment with PEG_4–*b*–PE_{25}. The difference in crystallinity was less than 2–3% in the case of the PLA based samples studied in the previous section (DSC results not shown here). In light of the collective results presented here, there is in our opinion no doubt that the trends are largely driven by interfacial effects.

4. Conclusions

The collective outcomes of this paper showed that the interfacial properties in cellulose-based bio-composites can be tailored through surface adsorption of polyethylene glycol (PEG) based amphiphilic block copolymers. The trends evidenced that the performance of the cellulose-based bio-composites could be remarkably enhanced by tuning both the nature of the block attached to the PEG block and the overall amphiphilicity (i.e. hydrophilic–lipophilic balance) of the block copolymers. Improvements in flexural modulus of up to 54% and 115% were observed in the PLA or HDPE based bio-composites after surface deposition and adsorption of the poly (ethylene glycol) based amphiphiles. The strong interfacial interactions formed across the fibre–matrix interface, such as intra- and inter-molecular hydrogen and van der Waals bonds, can be put forth as the main contributors to the performance improvement. At the very least, the methodology presented here offers a potentially greener alternative to other chemical methods presented in the literature as the deposition of aqueous amphiphilic emulsions or crystalline suspensions from solution onto the cellulosic substrate was carried out in a simple way using dip-coating. We believe that the outcomes from this study provide a technological template to significantly improve the performance of cellulose-based composite materials. We are currently using this concept to improve the performance of other functional composite materials.

Acknowledgements

The authors thank Alfred Deakin Prof. Xungai Wang at Deakin University for the financial support of this research project and Dr. Adam Taylor for his help on the SEM imaging.

Appendix A. Supplementary material

Supplementary data associated with this article can be found, in the online version, at http://dx.doi.org/10.1016/j.eurpolymj.2014.12.024.

References

[1] Mohanty AK, Misra M, Drzal LT. Compos Interfaces 2001;8:313–43.
[2] Satyanarayana KG, Arizaga GGC, Wypych F. Prog Polym Sci 2009;34:982–1021.
[3] Suddell BC, Rosemaund A. Industrial fibres: recent and current developments. In: Proceedings of the symposium on natural fibres, Rome; 2008.
[4] Bledzki AK, Gassan J. Prog Polym Sci 1999;24:221–74.
[5] Aziz SH, Ansell MP. Compos Sci Technol 2004;64:1219–30.
[6] Huda MS, Drzal LT, Mohanty AK, Misra M. Compos Sci Technol 2008;68:424–32.
[7] Rout J, Misra M, Tripathy SS, Nayak SK, Mohanty AK. Compos Sci Technol 2001;61:1303–10.
[8] Yan L, Mai Y-W, Lin Y. Compos Interfaces 2005;12:141–63.
[9] Kafi AA, Magniez K, Fox BL. Compos Sci Technol 2011;71:1692–8.
[10] Lee SG, Choi S-S, Park WH, Cho D. Macromol Symp 2003;197:89–100.
[11] Chu BY, Kwon MY, Lee SG, Cho D, Park WH, Han SO. J Soc Adhes Interf Korea 2004;5:9–16.
[12] Liston EM. Plasmas and surfaces – a practical approach to good composites. In: Akovali G, editor. The interfacial interactions in polymeric composites. Netherlands: Springer; 1993. p. 223.
[13] Brahmakumar M, Pavithran C, Pillai RM. Compos Sci Technol 2005;65(3–4):563–9.
[14] Kalia S, Kaith BS, Kaur I. Polym Eng Sci 2009;49(7):1253–72.
[15] Gandini A, Belgacem MN. Modifying cellulose fibre surfaces in the manufacture of natural fibre composites. In: Zafeiropoulos NE, editor. Interface engineering of natural fibre composites for maximum performance. Woodhead Publishing; 2001. p. 3–42.
[16] Folkes MJ. Short fibre reinforced thermoplastics. In: Bevis MJ, editor. Polymer engineering research studies. New York: Research Studies Press (Wiley); 1982.
[17] Prömper E. Natural fibre-reinforced polymers in automotive interior applications. In: Müssig, editor. Industrial applications of natural fibres. John Wiley & Sons; 2010. p. 421–36.
[18] Mohanty AK, Misra M, Drzal LT. Sustainable bio-composites from renewable resources: opportunities and challenges in the green materials world. J Polym Environ 2002;10(1–2):19–26.
[19] Magniez K, Voda AS, Kafi AA, Fichini A, Qipeng G, Fox BL. ACS Appl Mater Interfaces 2012;5:276–83.
[20] Hintermann M. Automotive exterior parts from natural fibres. In: Conference RIKO-2005, Hannover, Germany; 2005.
[21] English B. Wood fibre-reinforced plastics in construction. In: Falk RH, editor. Proceedings. The use of recycled wood and paper in building applications. Madison, Wisconsin; 1996. p. 79–81
[22] Yang J, Han C-R, Duan J-F, Xu F, Sun R-C. ACS Appl Mater Interfaces 2013;5:3199–207.
[23] Liang S, Wu J, Tian H, Zhang L, Xu J. ChemSusChem 2008;1:558–63.
[24] Colthrup NB, Daly LH, Wiberley SE. Introduction to infrared and Raman spectroscopy. 3rd ed. San Diego: Academic Press; 1990.
[25] Harrick NJ. Internal reflection spectroscopy. New York: John Wiley and Sons; 1967.
[26] Grøtli M, Gotfredsen CH, Rademann J, Buchardt J, Clark AJ, Duus JØ, et al. Comb Chem 2000;2:108–19.
[27] Gérard JF, Perret P, Chabert B. Study of carbon/epoxy interface (or interphase): effect of surface treatment of carbon fibres on the dynamic mechanical behavior of carbon/epoxy unidirectional composites. In: Ishida H, editor. Controlled interphases in composite materials. Netherlands: Springer; 1990. p. 449.
[28] Ko YS, Forsman WC, Dziemianowicz TS. Polym Eng Sci 1982;22:805–14.
[29] Chua PS. Polym Compos 1987;8:308–13.
[30] Afaghi-Khatibi A, Mai Y-M. Compos Part A – Appl Sci 2002;33(11):1585–92.
[31] Abidi N, Cabrales L, Haigler CH. Carbohydr Polym 2014;100:9–16.
[32] Lei Y, Wu Q, Clemons CM, Yao F, Xu Y. J Appl Polym Sci 2007;106:3958–66.